Process Modeling and Simulation Tools for Roll-to-Roll Nanomanufacturing

Kristianto Tjiptowidjojo[1], Andrew Cochrane[2], P. Randall Schunk[1,3]

[1]University of New Mexico, Chemical and Biological Engineering, Albuquerque, New Mexico, USA
[2]University of New Mexico, COSMIAC, Albuquerque, New Mexico, USA
[3]Sandia National Laboratories, Albuquerque, New Mexico, USA

1. INTRODUCTIONS

Modeling and simulation will play a critical role in nanomanufacturing process design and scale-up. Process models can guide tool design and defect-free process operation, as well as provide a means for uncovering physical mechanism causing defects.

Here we present our existing and developing capabilities of modeling and simulation of several nanomanufacturing processes. The software platform underpinning these capabilities is Goma 6.0, an open-source multi-physics finite element software developed by Sandia National Laboratories in partnership with industry [1]. The unit processes that we analyzed are slot-die coating, gravure printing, and nanoimprint lithography. They are described in Sections 2, 3, and 4 respectively.

2. SLOT-DIE COATING

Slot-die coating is a process in which liquid is extruded from a die onto a moving substrate to form a liquid film, as shown in Figure 1. The liquid bridge between the die and the substrate, commonly referred to as the "bead", is bounded by upstream and downstream capillary menisci. Typically a sub-ambient pressure, commonly called as "vacuum", is applied to stabilize the bead, especially when the wet thickness is less than half of the distance between the die and the substrate [2].

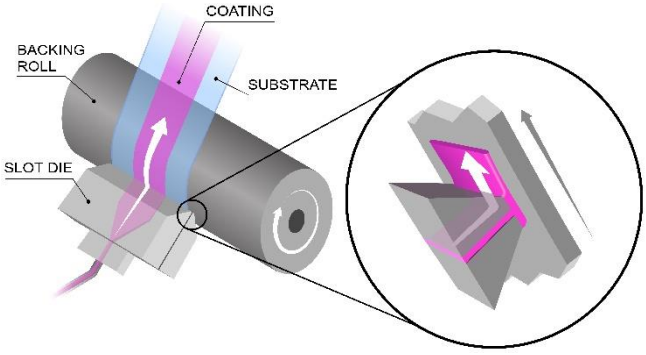

Figure 1: A schematic of slot-die coating process

Slot-die coating is one of the premier methods for precisely depositing film onto a moving substrate. Wet thickness in the order of 500 nm has been reported in tensioned-web-over-slot-diw modality [3]. The precision arises from premetered nature of the method, viz. the film thickness is set solely by flow rate and substrate speed. The quality of coating, however, heavily depends on liquid physical properties such as rheology (viscosity) and surface tension as well as operating conditions such as die-substrate gap and applied vacuum pressure. A set of liquid properties and operating conditions which enables uniform coating is referred as the "coating operability window".

The goal of our work is to predict the coating window, which is a region in operating parameter space in which uniform coatings can be achieved. Ideally, coating flows need to be steady, two-dimensional, and stable from disturbances. Thus, our modeling approach is based on solving steady-state two-dimensional conservation of momentum and mass-balance equations. Complications arise from moving boundaries introduced by free surface and contact lines are handled with arbitrary Lagrangian Eulerian (ALE) method [4].

The most relevant coating window for slot coating is defined by applied vacuum (high and low) and flowrate (or thickness). The applied vacuum needs to be within a certain range otherwise coating failure or defects would manifest. The range of applied vacuum leading to a successful coating forms the coating window. Based on experimental observation [5], onset of coating failure due to vacuum limits can be predicted from bottom meniscus location. Using those heuristics we were able to generate experimentally-validated coating windows shown in Figure 2. This work has been submitted for a publication [6]. A study of coating window limit bounded by flowrate, so-called low-flow limit, has also been published [7].

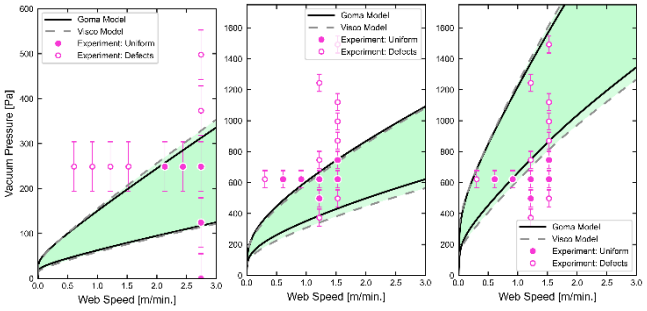

a. Dilute ink b. Concentrated ink 1 c. Concentrated ink 2

Figure 2: Slot-die coating window prediction of vacuum limits of fuel cell inks with 3 different shear viscosity rheologies

[3] Sandia National Laboratories is a multi-mission laboratory managed and operated by National Technology and Engineering Solutions of Sandia, LLC., a wholly owned subsidiary of Honeywell International, Inc., for the U.S. Department of Energy's National Nuclear Security Administration under contract DE-NA0003525.

3. GRAVURE PRINTING

Gravure printing is a contact printing technique with the pattern defined by recessed cells in a roller or a printing master, as shown Figure 3. It involves four steps: Filling the cells with ink, wiping the excess ink from the roll surface, transferring the ink to a substrate, and finally solidifying the ink on the substrate.

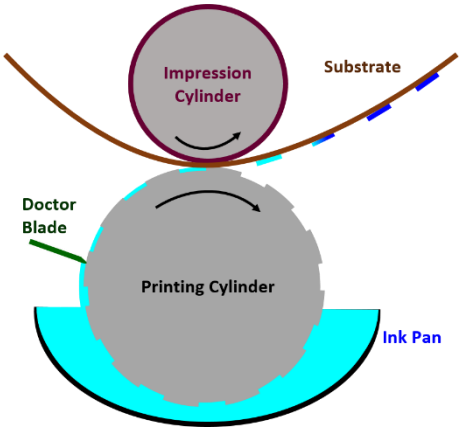

Figure 3: A schematic of gravure printing process

Gravure printing has garnered interest in flexible electronic industries due to its high-throughput and high-resolution advantage [8]. Resolution of sub-5 µm features has been reported at a speed of 1m/s, which is a significant improvement over other printing techniques viable for manufacturing of high performance devices, such as thin-film transistors [9]. The advancement is driven primarily by improvement of the tools used in each step. Here we focus on the use of modeling to improve the wiping step.

Our modeling approach addresses a common source of defects, viz. the wiping or doctoring process. Specifically, our model addresses the fluid-structure-interaction system between deformable blade and lubrication flow underneath [10]. The blade is treated as a Hookean elastic solid, in which three-dimensional Cauchy momentum equation is solved, while the liquid flow is modeled as a lubrication shell [11] to capture the disparately thin length scale between the blade tip and substrate. The model is used to optimize blade shape to yield thinnest residual film left behind while minimizing blade wear-out. A sample of prediction is shown in Figure 4. A detailed presentation of this work can be found in [12]. In summary, our model predicted the experimental results which were counter-intuitive in that the residual film thickness rises with printing speed, in opposite fashion of traditional blade coating.

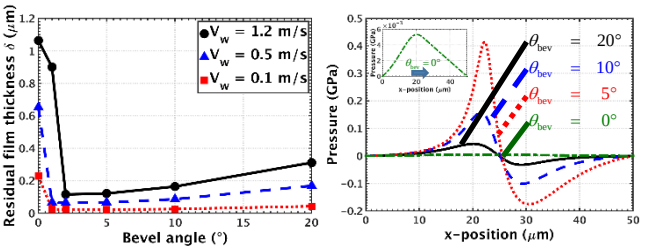

a. Residual film thickness as a function of bevel angle

b. Lubrication pressure profile underneath the blade tip

Figure 4: Prediction of residual film thickness left behind as a function of bevel angle of the blade tip and their corresponding lubrication pressure profile

4. NANOIMPRINT LITHOGRAPHY

Nanoimprint lithography (NIL) is a scalable method for manufacturing nanopatterned surfaces (feature size less than 100 nm) using a combination of capillary-driven imprinting and photo-polymerization processes. As shown in Figure 5, photoactive monomer drops are dispensed onto a substrate and then imprinted with nanopatterned mask (here shown in a roller modality). The combination of applied pressure and capillary forces exerted by the liquid bridges closes the gap between the surfaces as the drops merge and features fill. After capillary filling takes place, the nanopatterned monomer is cured with ultraviolet (UV) light to solidify the structure.

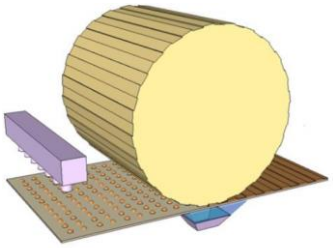

Figure 5: A schematic of nanoimprint lithography process [13].

Ideally, before the liquid is cured, all gas should be eliminated from the gap so that the liquid fills the template and the residual layer below the features is uniform over the print area. Gas trapping and residual layer thickness (RLT) variations are key limiters of process rate and yield, as trapped gas impedes feature filling and non-uniform residual layers adversely affect subsequent etching processes. The goal of our modeling work is to predict operating conditions that lead to uniform RLT and minimum trapped gas. Therefore, we focus on the droplet merging step without considering the capillary filling.

Just as in the gravure wiping modeling work described in Section 3, disparate length scale between the template-substrate gap and the patterned area demand the use of a reduced-order lubrication approximation of the flow. Our first attempt is to solve coupled Reynolds lubrication and level-set

advection equations [11] to model droplet merging flow in the gap. This approach is appropriate for a system with tens and hundreds of drops, but too computationally expensive for tens of thousands of drops typical in NIL processes.

We deployed a mixture-based theory of interacting continua to track the gas/liquid inventory for the full-scale case. That is we treated gas and liquid as disperse fluid phases in which the relative amount of each component is represented as volume fraction or saturation [14]. Flow of each component is governed with Darcy's law with appropriate modification of relative permeability in order to capture the correct dynamic seen in the flow visualization experiment. Figure 6 shows comparison of the two.

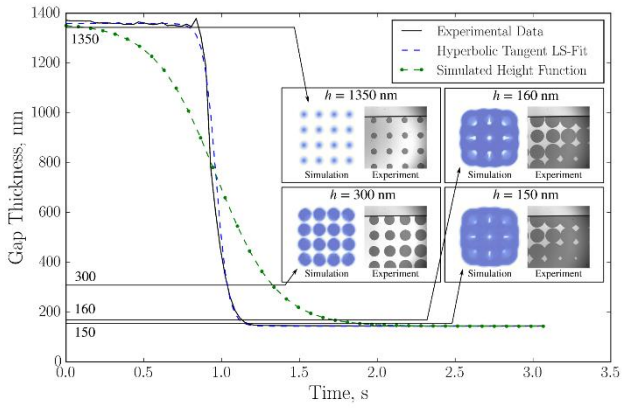

Figure 6: Comparison of Drops Merging State between Prediction and Flow Visualization as a Function of Gap Height

An important factor that is not considered in [14] is structural flexibility required for the template or the substrate in order to capture the effects of surface topology. We extended this work by including substrate deformation, and once again, due to disparate length scale between the pattern area and processing gap thickness typical of nanomanufacturing processes, we deployed efficient structural and lubrication shells simultaneously. A detailed description of this work can be found in [15].

5. CONCLUSION

We present a summary of our modeling approaches and results for several key nanomanufacturing processes. In each case we are able to capture important physics of the process and help guide process and tool development. The ability of coupling full three-dimensional (or two-dimensional) conservation of mass and momentum equations with reduced-order models such lubrication flow, multiphase disperse flow, and structural shells in Goma 6.0 enabled us to model the process at true machine scales.

ACKNOWLEDGMENTS

This work is supported primarily by the National Science Foundation under Cooperative Agreement No. EEC-1160494. Any opinions, findings and conclusions or recommendations expressed in this material are those of the author(s) and do not necessarily reflect the views of the National Science Foundation.

REFERENCES

[1] Schunk, P.R., et al., *Goma 6.0 - A Full-Newton Finite Element Program for Free and Moving Boundary Problems with Coupled Fluid/Solid Momentum, Energy, Mass, and Chemical Species Transport: User's Guide*, 2013

[2] Higgins, B. G., & Scriven, L. E.. *Chemical Engineering Science*, 1980 35(3), 673-682.

[3] Lin, F. H., Liu, C. M., Liu, T. J., & Wu, P. Y.. *Polymer Engineering & Science*, 2007 47(6), 841-851.

[4] Sackinger, P. A., Schunk, P. R., & Rao, R. R.. *Journal of Computational Physics*, 1996 125(1), 83-103.

[5] Romero, O. J., Suszynski, W. J., Scriven, L. E., & Carvalho, M. S.. *Journal of Non-Newtonian Fluid Mechanics*, 2004 118(2-3), 137-156.

[6] Creel, E. B., Tjiptowidjojo, K., Lee, J. A., Livingston K. M., Schunk, P. R., Bell, N. S., Serov, A., & Wood III, D. L.. *Journal of Colloids and Interface Science*, under revision.

[7] Malakhov, R., Tjiptowidjojo, K., & Schunk, *AIChE Journal*, 2019 65(6), e16593.

[8] Kang, H., Kitsomboonloha, R., Jang, J., & Subramanian, V.. *Advanced Materials*, 2012 24(22), 3065-3069.

[9] Grau, G., Cen, J., Kang, H., Kitsomboonloha, R., Scheideler, W. J., & Subramanian, V.. *Flexible and Printed Electronics*, 2016 1(2), 023002.

[10] Hariprasad, D. S., Grau, G., Schunk, P. R., & Tjiptowidjojo, K.. *Journal of Applied Physics*, 2016 119(13), 135303.

[11] Roberts, S. A., Noble, D. R., Benner, E. M., & Schunk, P. R.. *Computers & Fluids*, 2013 87, 12-25.

[12] Tjiptowidjojo, K., Hariprasad, D. S., & Schunk, P. R.. *Journal of Coatings Technology and Research*, 2018 15(5), 983-992.

[13] Jain A.. *Simulation of UV Nanoimprint Lithography on Rigid and Flexible Substrates*. 2016, Ph.D. Thesis, The University of Texas at Austin

[14] Cochrane, A., Tjiptowidjojo, K., Bonnecaze, R. T., & Schunk, P. R. *International Journal of Multiphase Flow*, 2018 104, 9-19.

[15] Cochrane, A., Tjiptowidjojo, K., Bonnecaze, R. T., & Schunk, P. R.. *Industrial & Engineering Chemistry Research*, 58(37), 2019 17424-17432.